PROCEEDINGS, 47th Workshop on Geothermal Reservoir Engineering
Stanford University, Stanford, California, February 7-9, 2022
SGP-TR-223

Data Mining Microseismicity Associated to the Blue Mountain Geothermal Site

Lucia F. Gonzalez[1], Ana C. Aguiar[2], Marianne Karplus[1]

[1] Department of Earth, Environmental and Resource Sciences, The University of Texas at El Paso, El Paso, TX, USA

[2] Lawrence Livermore National Laboratory, Livermore, California, USA

lfgonzalez5@miners.utep.edu, aguiarmoya1@llnl.gov, mkarplus@utep.edu

Keywords: Blue Mountain, Microseismicity, PageRank

ABSTRACT

Evidence of increasing microseismicity during geothermal power plant outages has been observed worldwide. Seismic studies in these areas provide several hypotheses mostly based on fault slip induction by changes in pore pressure. However, geological dissimilarities between regions halt assumptions of a unique stress mechanism for this phenomenon. Past methods like microearthquake location mapping have proved useful in delineating subsurface structure in these systems and understanding pathways for injection flow. Nevertheless, the stress changes triggering these events remain unclear in some cases. We apply a data mining technique, called PageRank, to assess microseismic event connectivity and evolution at the Blue Mountain geothermal site during 2017, a crucial first step to understand the origin of increased seismicity on-site during the annual power plant shutdown (September 18th) and other power plant operations. Here we compute direct (CC >= 0.6) and indirect (CC < 0.6, linkage stations >= 6) links to a reference event, a high PageRank event leading a seismic cluster. Cluster characterization results in several families comprised of unique microseismic events with similar waveform topology. In addition, traces from the indirect links within our identified families show a similar waveform pattern, confirming their belonging to the cluster. This study demonstrates the usefulness of PageRank to characterize microseismic events with similar physical properties, but also the advantages for a more robust cluster relocation analysis by affiliating low correlation events to the families, usually rejected by other methods.

1.INTRODUCTION

Rate changes of microseismicity in geothermal fields are crucial to understanding the effects of power plant operations and their disturbances to the stress environment of these systems. Additionally, the correlation and location of microseismic events can help identify the stimulated subsurface areas and discriminate between events triggered by different physical mechanisms. Multiple past studies have observed a relationship between extraction, cooling, and re-injection of fluids and the rates of microseismicity in the subsurface (Asanuma *et al*, 2007; Buijze *et al*, 2019), mostly due to the changes in pore pressure (Ellsworth, 2013; Zhai *et al*, 2019; Maurer *et al*, 2020). Theoretically, in active geothermal sites, the injection of heated fluids in heavily faulted areas causes the ambient fluid pore pressure to increase and the effective stress to decrease, inducing fault slip seismicity (Cardiff *et al*, 2018). However, an increase in microseismic events has also been linked to the cease of power plant operations (Davatzes *et al*, 2013). This is the case of the Blue Mountain geothermal site, located in Humboldt County, Nevada. Owned by Cyrq Energy, the Blue Mountain geothermal site first started energy production in 2009. It currently counts with six production wells and seven injection wells to optimize the production rate. Here, a significant increase in the number of events is persistently observed during the annual maintenance power plant shutdowns (Templeton *et al*, 2017), where all the production wells go offline and the injection pump is shut off.

Although past studies have provided correlation evidence between microseismicity and geothermal energy operations, the stress mechanisms causing an increase of events after power plants cease operations have not been accurately determined. To understand this phenomenon, event cluster discrimination and characterization can be used as an initial step to help image and understand stress changes in the system based on on-site geological processes and power plant activity. We use an algorithm created by Google, called PageRank, adapted to assess microseismic events connectivity by using waveform cross-correlation. PageRank links events to families led by a high-ranked microseismic event (Aguiar and Myers, 2014). We apply this method to Blue Mountain data for 2017, detected by an STA/LTA approach, to identify event families most likely associated with the same processes at depth. Characterization of microseismic event families and their future relocations will serve as a tool to understand changes in the subsurface by power plant outages and their effect on seismicity rates. Ultimately, identifying the impact on the stress environment (Majer *et al*, 2007) during geothermal plant shutdowns, a fundamental knowledge gap, can help improve geothermal management and production, potentially impacting renewable energy services worldwide.

2. DATA SET

The Blue Mountain Geothermal site has a permanent seismic network initially deployed in 2015. Between December 2015 and August 2016, the network comprised eight seismic stations (BM01 to BM08) that consist of two 3-component borehole geophones and six 3-component surface shallow-buried geophones with digitizers recording at 250 Hz (Matzel, 2020). In September 2016, two more 3-component geophones (station BM09 and BM10) were deployed and added to the permanent network to increase area coverage of recorded data generated by natural phenomena and the energy production operations on site (Figure 1).

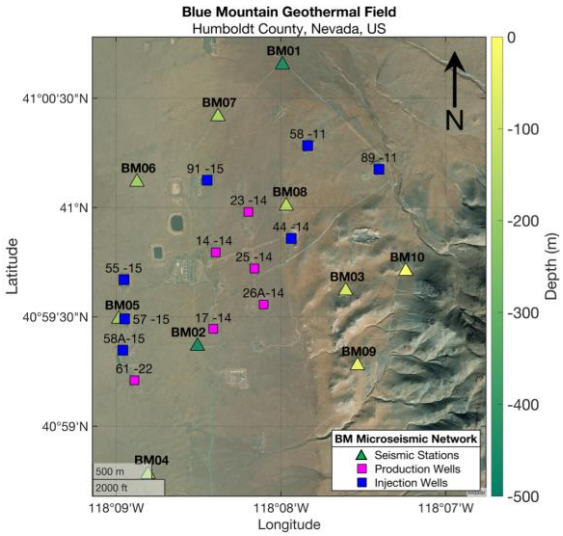

Figure 1: Map of the Blue Mountain Geothermal Field in Nevada, illustrating the permanent seismic network and well locations that have been used for multiple studies. A total of 10 seismic stations (triangles), six production wells (pink squares), and seven injection wells (blue squares) are shown. Color bar indicates the buried depth of the seismic stations. For this analysis, we use all the production and injection wells, and seismic stations except for BM05 and BM08.

We focus on data from 2017 with 498 microseismic events detected using a Short-Term/Long Term Algorithm (STA/LTA) approach applied to the continuous data (Templeton *et al.* 2017) (Figure 2). We excluded station BM05 and BM08 from the analysis due to no data recorded by the instruments during this year.

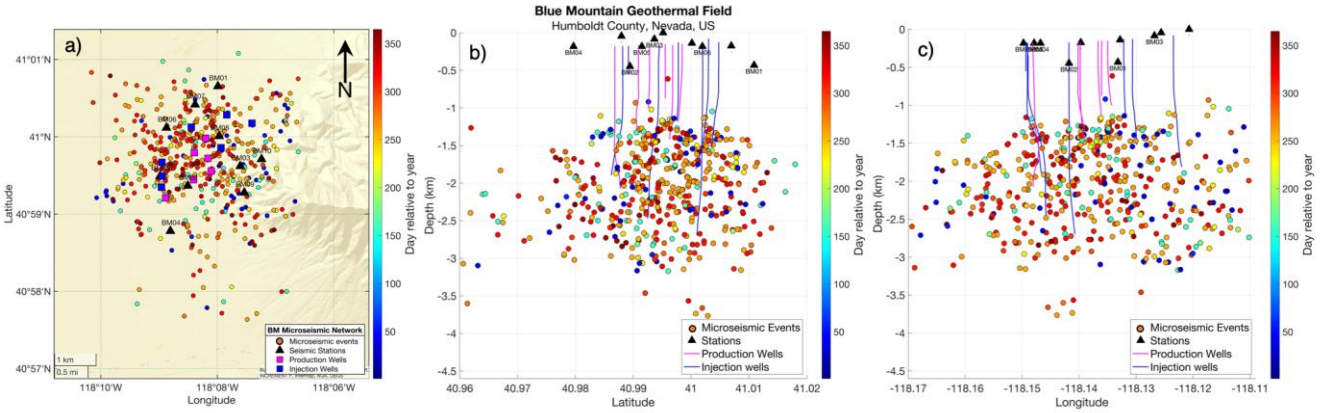

Figure 2: a) Map view, b) elevation vs latitude profile, and c) elevation vs longitude profile to illustrate the subsurface of Blue Mountain and microseismic activity during 2017. In total, the seismometers captured 498 microseismic events (circles). Seismic stations (black triangles) are illustrated for location reference. Color bar represents the day that the event was recorded, transitioning from dark blue for the initial days of the year to dark red for the last days of the year. Figures b) and c) depict production wells with pink lines and injection wells with blue lines to show their extent under the surface.

2.1 Power Plant Shutdown

As mentioned in Templeton et al. (2017), an increase in seismicity at Blue Mountain was observed during the April 2016 power plant shutdown. Likewise, a spike in seismicity can be observed in 2017 during the annual maintenance power plant outage in September 2017. The outage started with the injection pump shutting off, followed by all the production wells going offline. The instruments recorded a significant increase of events following this shutdown and later seismicity rapidly decreased as operations resumed, as shown in Figures 3 and 6.

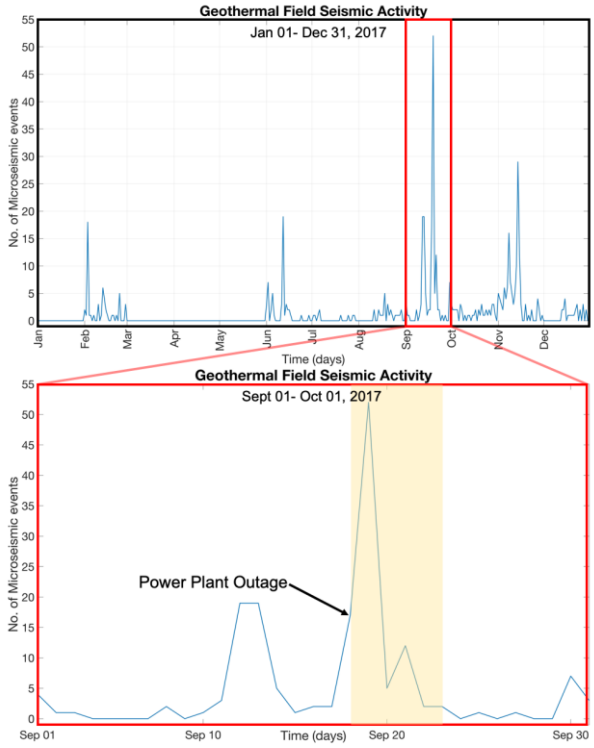

Figure 3: Microseismicity timeline of Blue Mountain in 2017. Top figure shows the daily occurrence of microseismic events, highlighting September (red rectangle), when the scheduled power plant outage occurred. Bottom figure shows seismic activity in September, where the colored vertical bar highlights the outage and post-shutdown dates. The scheduled outage, September 18th, consisted of the injection pump shut off and the production wells going offline. As observed, a dramatic increase in seismicity occurred during this period.

3. METHODOLOGY AND RESULTS

PageRank was originally developed by Google to optimize their search engine and display websites by hierarchy order (Brin and Page, 1998). The algorithm produced a ranking for a webpage computed from the number of links between websites and the relevance of these links to the researched topic. Aguiar and Beroza (2014) adapted this algorithm for seismic data mining based on waveform cross-correlation linkage. High-ranked seismic events are defined as a reference event, an event with the most links to other events in a sequence and leading an event family. To populate the families, links are identified in two manners: direct links to a reference event by meeting the waveform cross-correlation threshold criteria and indirect links by meeting the same threshold criteria through an event directly linked to the reference event (Aguiar and Beroza, 2014). Aguiar and Myers (2017; 2018) later applied this algorithm to microseismic data and showed that having the ability to include indirectly linked events in the analysis, relocation and event characterization can be significantly improved.

Here we apply PageRank to the Blue Mountain events from 2017 shown in Figure 2. Currently, two families have been identified comprising a different number of events. We first obtained direct and indirect links for both families based on a set waveform cross-correlation threshold (CC>=0.6), followed by anchoring events to the family if they were linked to the reference event by six or more stations. Results for both families, 57 and 243 (reference event number), are shown in Figures 4 and 5, respectively.

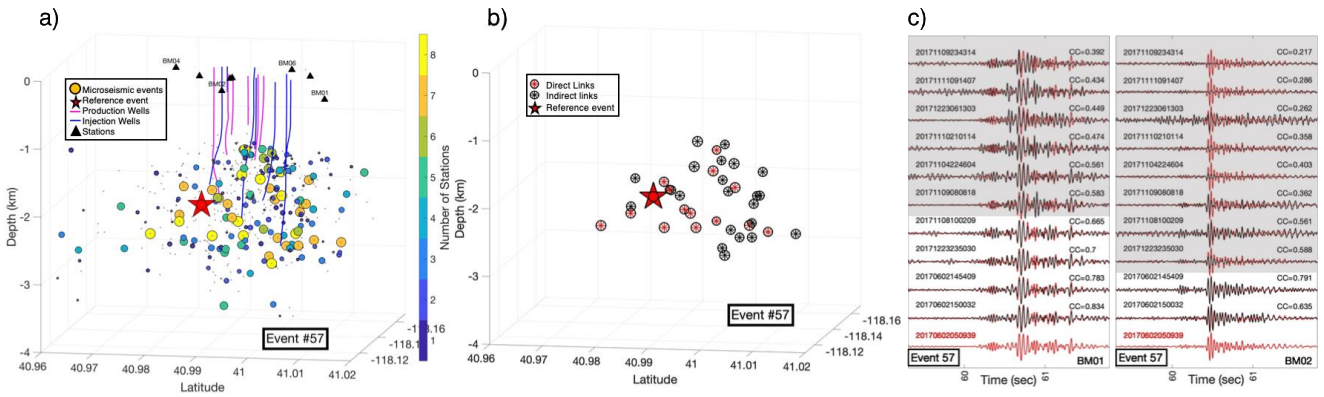

Figure 4: Event family led by reference event 57 (red star). a) Number of stations linking microseismic events to the family. Small circles and cold colors represent a low number of stations, while warmer colors and larger circles represent a more significant number of stations. In addition, production (pink lines) and injection (blue lines) wells are shown. b) Direct and indirect links connected to the reference event by six or more stations. c) Traces from the direct (white background) and indirect links (gray background) at two of our best stations. The reference event (red line) is superimposed on the other traces (black lines) to observe waveform correlation. The color of traces is not related to Figure 4b. As observed, indirect links have a similar waveform to the identified direct links, suggesting that these events can also be used for the future relocation of this family.

In event family 57, we can observe that 36 events are linked to the reference event by six or more stations (Figure 4a). From those events, 14 are identified as direct links (CC>= 0.6), while the remaining 22 are identified as indirect (CC< 0.6) as shown in Figure 4b. Traces of direct links exhibit a similar or almost identical waveform pattern, confirming that they belong to the same family. However, as observed, traces from indirect links also have a similar waveform pattern to those identified as direct links (Figure 4c). Despite these events being secluded from the family by threshold criteria, these results show that they belong to this cluster and can be used for future relocation.

Figure 5 shows similar results for the second family where direct and indirect links are confirmed to be from the same cluster due to similar waveform pattern. We identify a total of 23 links connected to reference event 243 by six or more stations (Figure 5a). From these events, 17 are direct links and 6 are indirect links (Figure 5b).

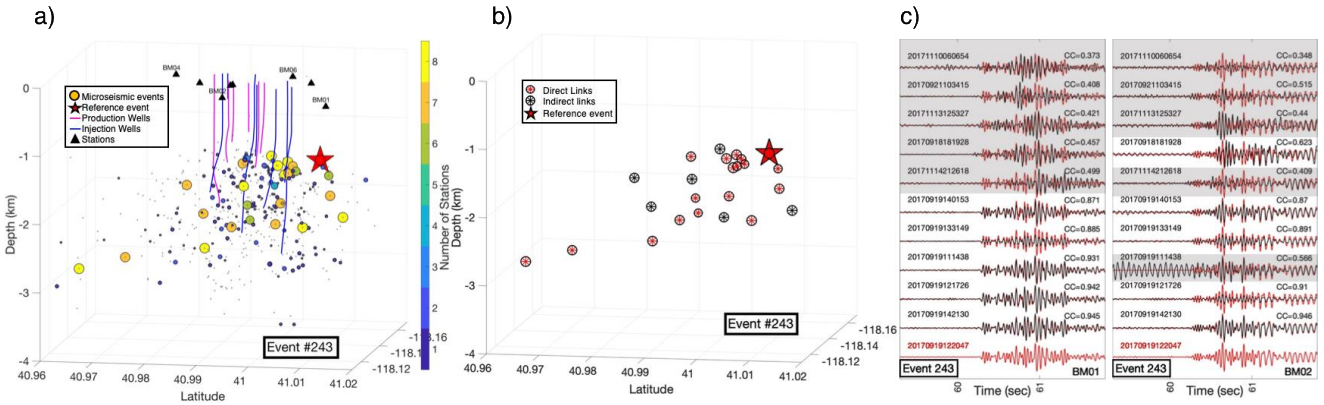

Figure 5: Event family led by reference event 243 (red star). a) Stations linking the events to the reference event. The stations are represented by size and color, where small circles and colder colors indicate a small number of stations, while large circles and warmer colors represent a larger number of stations. b) Identified direct and indirect links. c) Traces from direct (white background) and indirect links (gray background) shown in Figure 5b.

We compare events within these two families to events that occurred during the annual shutdown, and even though events within the family of event 57 do not seem to coincide with this time frame, we do find matching locations between events from family 243 and seismicity triggered during the power plant shutdown, suggesting that this family was produced during the outage. Figure 6 shows locations for events within both families (black) and the events within the shutdown timeframe colored by date.

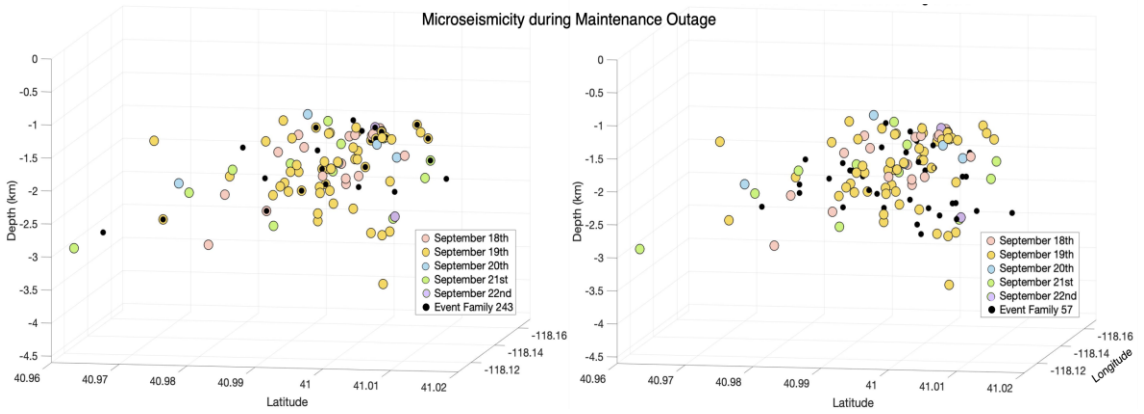

Fig 6: Location of microseismic events detected during the 2017 annual outage (pastel colored circles) and events within family 243 and 57 (black circles). Pastel colors represent the detection date. As noticed, some events from family 243 overlie the location of events related to the shutdown, which gives us confidence that this cluster belongs to the phenomenon discussed above.

4. CONCLUSIONS AND FUTURE WORK

We use data recorded at the Blue Mountain geothermal field in 2017 to test PageRank for resolving microseismicity cluster characterization. We have currently identified two event families on the northern side of the field, comprising unique microseismic events. Events within these families present similar waveforms suggesting similar event topology and geological mechanism at depth, while one of the families occurs during the annual power plant outage suggesting this family could be associated to subsurface stress changes caused by the shutdown. In addition, trace evidence from direct and indirect links indicates that events with a low correlation and linked to the reference event by six or more stations present a highly similar waveform to high correlation events, confirming cluster affiliation and noticeably expanding family dimensions.

Further analysis of families within the data set will help us understand the evolution in space and time of the 2017 microseismic seismicity at the Blue Mountain geothermal field. This will also allow us to further explore the relocation of events by taking advantage of family similarities. Most existing relocation methods require a vast number of P and S phase arrivals for highly accurate results. We will use PageRank results to obtain differential arrival times within families and relocate events. Future relocation of these clusters will help understand the faulting system at Blue Mountain and stress mechanisms triggering events due to halted flow of injection fluids, a persistent phenomenon in this geothermal field. Eventually, identifying stress mechanisms triggering seismicity during power plant operations will serve as a powerful tool to understand subsurface behavior and properly optimize and manage geothermal energy production.

ACKNOWLEDGEMENTS

This work performed under the auspices of the U.S. Department of Energy by Lawrence Livermore National Laboratory under Contract DE-AC52-07NA27344. LLNL-CONF-831033

REFERENCES

Aguiar, A.C., and Beroza, G. C.: Pagerank for earthquakes. Seismological Research Letters, 85(2), (2014), 344-350.

Aguiar, A. C. and Myers S. C.: Microseismic Event Relocation Based on PageRank Linkage at the Newberry Volcano Geothermal Site, Proceedings, 42th Workshop on Geothermal Reservoir Engineering, Stanford University, Stanford, California, February 13-15 (2017).

Aguiar, A.C., and Myers, S. C.: Microseismic Event Relocation based on PageRank linkage at the Newberry Volcano Geothermal Site, Bulletin of the Seismological Society of America, 108(6), (2018), 3656-3667.

Asanuma, H., Kumano, Y., Hotta, A., Schanz, U., Niitsuma, H., and Häring, M.: Analysis of microseismic events from a stimulation at Basel, Switzerland, GRC Transactions, 31, (2007), 265–269.

Brin, S. and Page, L.: The anatomy of a large-scale hypertextual Web search engine, Computer Networks and ISDN Systems, 30, (1998), 107-117.

Buijze, L., Bijsterveldt, L., Cremer, H., Jaarsma, B., Paap, B., Veldkamp, J.G., Wassing, B., Van Wees, J., van Yperen, G., ter Heege, J.: Induced seismicity in geothermal systems: Occurrences worldwide and implications for the Netherlands, European Geothermal Congress 2019, Den Haag, The Netherlands, June 11-14, 2019.

Cardiff, M., Lim, D. D., Patterson, J. R., Akerley, J., Spielman, P., Lopeman, J., Walsh, P., Singh, A., Foxall, W., Wang, H.F., Lord, N. E., Thurber, C. H., Fratta, D., Mellors, R. J., Davatzes, N. C., Feigl, K.L.: Geothermal production and reduced seismicity: Correlation and proposed mechanism, Earth and Planetary Science Letters, 482, (2018), 470-477.

Davatzes, N.C., Feigl, K.L., Mellors, R.J., Foxall, W., Wang, H.F., Drakos, P.: Preliminary Investigation of Reservoir Dynamics Monitored Through Combined Surface Deformation and Micro-Earthquake Activity: Brady's Geothermal Field, Nevada, Proceedings, 38th Workshop on Geothermal Reservoir Engineering, Stanford University, Stanford, California, February 11-13 (2013).

Ellsworth, W.L.: Injection-induced earthquakes, Science, 321, (2013), 142.

Huang, L., Gao, K., Huang, Y., and Cladouhos, T.: Anisotropic Seismic Imaging and Inversion for Subsurface Characterization at the Blue Mountain Geothermal Field in Nevada, Proceedings, 43rd Workshop on Geothermal Reservoir Engineering, Stanford, California, February 12-14, (2018).

Majer, E. L., Baria, R., Stark, M., Oates, S., Bommer, J., Smith, B., Asanuma, H.: Induced seismicity associated with Enhanced Geothermal Systems, Geothermics,36, (2007),185-222.

Matzel, E.M.: Using Seismic Interferometry to Identify and Monitor Fluids in Geothermal Systems, Proceedings, World Geothermal Congress 2020, Reykjavik, Iceland, April 26-May 2 (2020).

Maurer, V., Gaucher, E., Grunberg, M., Koepke, R., Pestourie, R., Cuenot, N.: Seismicity induced during the development of the Rittershoffen geothermal field, France, Geothermal Energy 8, 5, (2020).

Matzel, E.M.: Using Seismic Interferometry to Identify and Monitor Fluids in Geothermal Systems, Proceedings, World Geothermal Congress 2020, Reykjavik, Iceland, April 26- May 2, (2020).

Swyer, Michael & Uddenberg, Matt & Nordin, Yini & Cladouhos, T. & Petty, Susan. (2016). New Injection Strategies at Blue Mountain, Nevada Through Tracer Test Analysis, Injection- Production Correlation, and an Improved Conceptual Model.

Templeton, D.C., Matzel, E.M., and Trenton, T.C.: Evolution of Microseismicity at the Blue Mountain Geothermal Site, GRC Transactions, 41, (2017) 1752-1755.

Zhai, G., Shirzaei, M., Manga, M., Chen, X.: Pore-pressure diffusion, enhanced by poroelastic stresses, controls induced seismicity in Oklahoma, Proceedings of the National Academy of Sciences of the United States of America, (2019).